Memoirs of the Faculty of Engineering, Nagoya University
Vol. 40, No. 2 (1988) –Research Report–

NUMERICAL STUDY ON GAS-SOLID TWO-PHASE NOZZLE AND JET FLOWS

A. Koichi HAYASHI, Minoru MATSUDA
and Toshi FUJIWARA

Department of Aeronautical Engineering

(Received October 31, 1988)

Abstract

The solid particle laden two-phase nozzle and jet flows are studied numerically applying a Flux Vector Splitting – Upwind scheme for a gas-phase and a Lagrangian method for a solid-phase to solve the two-phase Euler equations. The Eulerian formulation for the two-phase flow problem is simpler in the theoretical structure and more economical in the computational time than the Lagrangian formulation. However the boundary conditions on the center axis of symmetry give a difficulty with explaining the physical phenomena on the axis. Hence in the nozzle and jet flows the Lagrangian way of calculations is applied for the solid phase to avoid the boundary problems.

The numerical results of the solid particle flow of a nozzle and jet simulate an experimental result to validate the developed code.

Introduction

The multi-phase flow has been studied step-by-step for a long time.[1)-6)] The purpose of its study has many varieties such as a safety of coal mine explosions, a sedimentation problem in river, a two-phase exaust problem in a solid rocket booster, and so on. The recent strong needs of the two-phase flow studies for solid and liquid rockets motivate a numerical simulation of the two-phase nozzle and jet flows. One of the main interests in their flows is a radiation signature from the two-phase exhaust gases of a solid rocket motor, which damages the boosters and their equipment. In the nozzle flow solid particles deteriorate the nozzle performance and cause a damage to the nozzle wall.

The present study shows the numerical analysis of the gas-solid two-phase nozzle and jet flows to verify the numerical code and to understand the solid particle effects on the two-phase flow properties. The calculation is performed using a non-steady two-dimensional or axisymmetric Euler as well as Lagrangian type equations, which have a quasi-conserved form. The Flux Vector Splitting – Upwind scheme for the gas-phase and the Lagrangian scheme for the solid-phase in nozzle and jet flows are used for calculations with the first order accuracy to gas-phase and the second order accuracy to solid-phase. Parameters associated with the two-phase drag force and heat transfer are given by the functions of the particle Reynolds number and the particle Mach number.

Governing Equations

In order to set up the governing equations for the gas-solid two-phase flow, the following assumptions are considered.

(1) Mass is conserved in the gas, solid, and their mixture phases.
(2) Mixture is adiabatic and its total energy is conserved.
(3) Gas is perfect, chemically frozen, and inviscid.
(4) There are collisions between solid particles when the Lagrangian type particle equations are considered and no collisions when the Eulerian type particle equations are considered.
(5) The solid particle specific heat is independent of temperature, hence the temperature profile within the solid particle is homogeneous.
(6) The solid particle density is about thousand times larger than the gas density and its volume is negligibly small comparing with gas.
(7) The solid particle surface is smooth and its shape is uniformly sphere.
(8) There is no external force, such as the gravitational force, the Basset force, the lift force and etc.

The assumptions described above are minimum counts and some more assumptions may be necessary.

The two-phase Euler equations used for the gas-phase in the nozzle and jet flows are unsteady, quasi-conservative and cylindrically symmetry and are shown as follows:

$$\frac{\partial U}{\partial t}+\frac{\partial F}{\partial x}+\frac{\partial G}{\partial r}+H=0 \tag{1}$$

where U, F, G, and H are

$$U=\begin{bmatrix} \rho \\ \rho \mathrm{u} \\ \rho \mathrm{v} \\ e \\ \rho_{\mathrm{s}} \\ \rho_{\mathrm{s}}\mathrm{u}_{\mathrm{s}} \\ \rho_{\mathrm{s}}\mathrm{v}_{\mathrm{s}} \\ e_{\mathrm{s}} \end{bmatrix} \qquad F=\begin{bmatrix} \rho \mathrm{u} \\ \rho \mathrm{u}^2+\rho \\ \rho \mathrm{u}\mathrm{v} \\ (e+p)\mathrm{u} \\ \rho_{\mathrm{s}}\mathrm{u}_{\mathrm{s}} \\ \rho_{\mathrm{s}}\mathrm{u}_{\mathrm{s}}^2 \\ \rho_{\mathrm{s}}\mathrm{u}_{\mathrm{s}}\mathrm{v}_{\mathrm{s}} \\ e_{\mathrm{s}}\mathrm{u}_{\mathrm{s}} \end{bmatrix} \qquad G=\begin{bmatrix} \rho \mathrm{v} \\ \rho \mathrm{u}\mathrm{v} \\ \rho \mathrm{v}^2+\rho \\ (e+p)\mathrm{v} \\ \rho_{\mathrm{s}}\mathrm{v}_{\mathrm{s}} \\ \rho_{\mathrm{s}}\mathrm{u}_{\mathrm{s}}\mathrm{v}_{\mathrm{s}} \\ \rho_{\mathrm{s}}\mathrm{v}_{\mathrm{s}}^2 \\ e_{\mathrm{s}}\mathrm{u}_{\mathrm{s}} \end{bmatrix}$$

$$H=\begin{bmatrix} 0+\dfrac{\rho \mathrm{v}}{r} \\ \rho_s A_s(\mathrm{u}-\mathrm{u}_s)+\dfrac{\rho \mathrm{u}\mathrm{v}}{r} \\ \rho_s A_s(\mathrm{v}-\mathrm{v}_s)+\dfrac{\rho \mathrm{v}^2}{r} \\ \rho_s A_s B_s+\dfrac{(e+\rho)\mathrm{v}}{r} \\ 0+\dfrac{\rho_s \mathrm{v}_s}{r} \\ -\rho_s A_s(\mathrm{u}-\mathrm{u}_s)+\dfrac{\rho_s \mathrm{u}_s \mathrm{v}_s}{r} \\ -\rho_s A_s(\mathrm{v}-\mathrm{v}_s)+\dfrac{\rho_s \mathrm{v}_s^2}{r} \\ -\rho_s A_s B_s+\dfrac{e_s \mathrm{v}_s}{r} \end{bmatrix}$$

$$e=\rho\left[c_v T+\frac{\mathrm{u}^2+\mathrm{v}^2}{2}\right],\quad e_s=\rho_s\left[c_s T_s+\frac{\mathrm{u}_s^2+\mathrm{v}_s^2}{2}\right] \tag{2}$$

and

(3)

A_s and B_s in Eq. (2) are the parameters related with the drag force and heat transfer between two phases respectively and are shown in the forms:

$$A_s=\frac{9}{2}\left[\frac{\mu_g \bar{C}_D}{m_s r_s^2}\right];\quad \bar{C}_D=\frac{C_D}{C_{D0}}\ (C_{D0}=\text{the stokes drag coefficient}) \tag{4}$$

and

$$B_s=\mathrm{u}_s(\mathrm{u}-\mathrm{u}_s)+\mathrm{v}_s(\mathrm{v}-\mathrm{v}_s)+\frac{2c_p Nu(T_s-T)}{3\bar{C}_D Pr} \tag{5}$$

Among the parameters used in Eqs. (3)–(5) C_p is the specific heat of gas at a constant pressure, C_v the specific heat of gas at a constant volume, C_s the specific heat of solid particle, m_s the concentration of solid particle, r_s the radius of solid particle, and μ_g the dynamic viscosity of gas.

The solid-phase Lagrangian type equations are:

$$\frac{du_s}{dt}=\frac{3}{8}\frac{C_D}{r_s m_s}\rho\,(u-u_s)\,|u-u_s|, \tag{6}$$

$$\frac{dv_s}{dt}=\frac{3}{8}\frac{C_D}{r_s m_s}\rho\,(v-v_s)\,|v-v_s|, \tag{7}$$

$$\frac{dT_s}{dt}=\frac{3}{r_s{}^2 m_s}\frac{c_p}{c_s}\frac{\mu_g Nu}{P_r}(T-T_s), \tag{8}$$

$$\frac{dx_s}{dt}=u_s, \tag{9}$$

$$\frac{dr_s}{dt}=v_s \tag{10}$$

Drag Coefficient C_D and Nussetlt Number Nu

The drag coefficient C_D and Nusselt number Nu in Eqs. (4)–(8) are the important parameters in two-phase flows. The stokes law or its modified drag coefficient, which is a function of the relative Reynolds number only, was used in the two-phase flow problem in the early 1970s. However Carlson and Hogland[7] have already developed and used the empirical expression for the drag coefficient of a spherical particle as a function of the relative Mach number as well as the relative Reynolds number in studying the rocket nozzle problem.

Later Walsh (1975)[8] obtained an empirical expression of the drag coefficient based on the ballistic range experiments.

The drag coefficient by Henderson (1976)[9] is applied to the present numerical simulation since the Henderson's formula is based on the data of Walsh and can be applied to the compressible flow. The Henderson's drag coefficient is:

$M \leq 1.0$

$$C_D=24\left[Re_s+S_s\left[4.33+\frac{3.65-1.53T_s/T}{1+0.353T_s/T}\right]\exp\left[-\frac{0.247Re_s}{S_s}\right]\right]^{-1}$$
$$+\exp\left[-\frac{0.5M_s}{\sqrt{Re_s}}\right]\left[\frac{4.5-0.38\left[0.03Re_s+0.48\sqrt{Re_s}\right]}{1+0.03Re_s+0.48\sqrt{Re_s}}+0.1M_s^2+0.2M_s^8\right]$$
$$+0.6S_s\left[1-\exp\left[-\frac{M_s}{Re_s}\right]\right] \tag{11}$$

$M \geq 1.75$

$$C_D = \frac{0.9 + \frac{0.34}{M_s^2} + 1.86\sqrt{\frac{M_s}{Re_s}}\left[2 + \frac{2}{S_s^2} + \left[\frac{1.058}{S_s}\right]\sqrt{\frac{T_s}{T}} - \frac{1}{S_s^4}\right]}{1. + 1.86\sqrt{\frac{M_s}{Re_s}}} \tag{12}$$

$1.0 \leq M \leq 1.75$

$$C_D(M_s, Re_s) = C_D(1.0, Re_s) + \frac{4}{3}(M_s - 1.0)[C_D(1.75, Re_s) - C_D(1.0, Re_s)]. \tag{13}$$

The Nusselt number for the gas-solid two-phase flow has not been studied as much as the drag coefficient since it is difficult to measure the heat transfer in a small particle. The Nusselt number used in the present calculation is the one formulated by Carlson and Hogland[7] as follows:

$$Nu = \frac{2 + 0.459 Re_s^{0.55} Pr^{0.33}}{1. + 3.42\left[\frac{M_s}{Re_s Pr}\right](2. + 0.459 Re_s^{0.55} Pr^{0.33})} \tag{14}$$

The parameters used in Eqs. (4)–(14) are the Prandtl number of gas Pr=0.75, the relative Reynolds number based on the dynamic viscosity of gas $Re_s = 2(\Delta V) r_s \rho / \mu_g$, the relative velocity $\Delta V = \sqrt{(u-u_s)^2 + (v-v_s)^2}$, he relative frozen Mach number $M_s = \Delta V/a$ (a; the speed of sound of gas), the molecular velocity ratio $S_s = M_s\sqrt{\frac{\gamma}{2}}$, the dynamic viscosity of gas $\mu_g = 17.17 x 10^{-6} (T/273.)^{0.77}$.

Numerical Scheme

In order to solve the system of nonlinearly coupled, unsteady, cylindrically-coordinated governing equations, Eqs. (1)–(3) and (6)–(10), the finite difference approximations are employed to linearize the transport equations. Originally a first (gas-phase) and second (solid-phase) order Flux Vector Splitting – Upwind schemes[10),11)] and a curvilinear coordinated grid system are utilized to the two-phase nozzle flow. After the difficulty with boundary conditions on the symmetric axis is found, a Lagrangian type of approach is applied for the solid-phase calculation.

Flux Vector Splitting – Upwinding Scheme[10]

The first- and second-order accuracy upwinding schemes are used for the gas-phase in the nozzle and jet flows in a Flux Split fashion. The governing equation is finitely differentiated as a predictor;

$$U_{i,j}^{\overline{n+1}} = U_{(i,j)}^{n} - \frac{\Delta t}{\Delta x}[(F_{i+1,j}^{+})^{n} - (F_{i,j}^{+})^{n}] - \frac{\Delta t}{\Delta x}[(F_{i,j}^{-})^{n} - (F_{i-1,j}^{-})^{n}] - \Delta t H_{i+j}^{n} \tag{15}$$

where

$$F^{+} = \frac{1}{2}(F + \hat{F}),\ F^{-} = \frac{1}{2}(F - \hat{F})$$
$$\hat{F} = U|u|\ \ (\hat{G} = U|v|) \tag{16}$$
$$F = AU,\ A = R\Lambda R^{-1}.$$

The Λ is a matrix of absolute eign values. In order to keep the equation specially with the second order accuracy, the following equation is considered as a corrector to the above equation in the case of the solid-phase flow calculation;

$$U_{i}^{n+1} = \frac{1}{2}(U_{i}^{n} + U_{i}^{\overline{n}}) - \frac{\Delta t}{2\Delta x}(F_{i+2}^{-} - 2F_{i+1}^{-} + F_{i}^{-})^{n} + \frac{\Delta t}{2\Delta x}(F_{i}^{+} - 2F_{i-1}^{+} + F_{i-2}^{+})^{n} - \frac{\Delta t}{2\Delta x}(F_{i+1}^{-} - F_{i}^{-})^{\overline{n+1}} - \frac{\Delta t}{2\Delta x}(F_{i}^{+} - F_{i-1}^{+})^{\overline{n+1}} - \Delta t H^{\overline{n+1}} \tag{17}$$

The time step for the calculation is determined by the CFL condition using the Courant number, C, as follows:

$$C = \frac{\Delta t}{\Delta x}\left[a + \sqrt{u^2 + v^2}\right] \tag{18}$$

The Courant number is kept unity for the usual flow calculation and that of less than 0.6 is used for the present case.

The Lagrangian Eqs. (6)–(10) are simply described by the centered finite difference scheme.

Grid Systems and Initial and Boundary Conditions

Grid Systems

Typical examples of the grid system for the nozzle and jet flows utilized in the present calculation are shown in Fig. 1. An algebraical grid formation; a boundary fitted coordination, is used for the converging-diverging nozzle flow with the grid points 58×170 and for the jet flow with the grid points 30×130. The grids are clustered near the nozzle throat and diverging section.

(a)

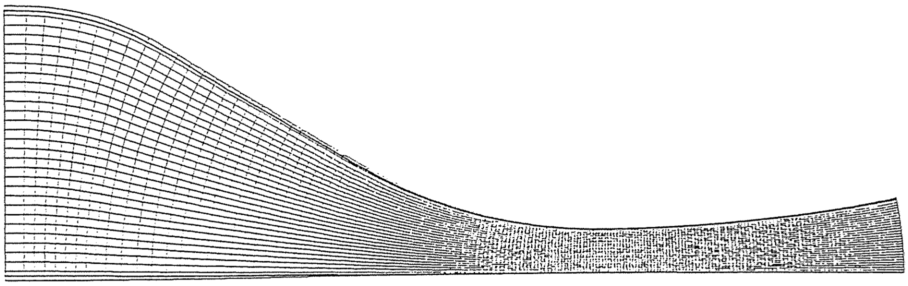

(b)

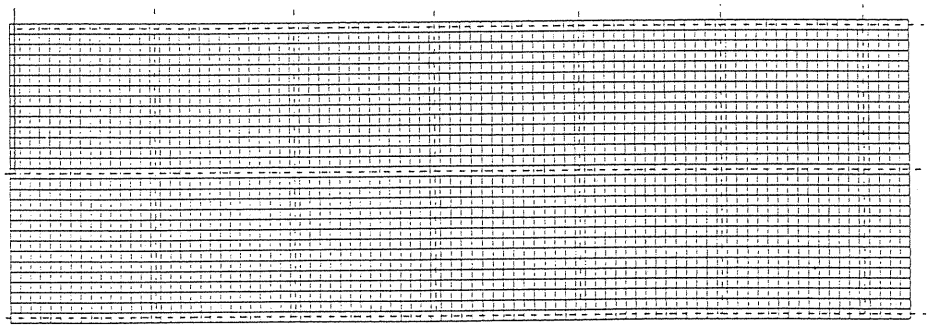

Fig. 1. Grid systems for (a) the nozzle (58×170) and (b) jet (30×130) flows used in the present calculation.

Initial Conditions

The initial condition for the nozzle flow problem is given by the solution of an axisymmetric gaseous flow, which is obtained by calculating the one-dimensional combustion chamber flow. The solid particle density is distributed initially over the computational domain by the amount multiplying the gaseous density by the solid particle loading ratio. The initial condition for the jet flow is given by the solution of the nozzle flow problem.

Boundary Conditions

The two-phase nozzle and jet flows are calculated until the stedy state condition is reached; the residual of the change in density or pressure in the whole flow field becomes 10^{-5} or less. The boundary conditions at the wall and at the center axis are set to be the mirror reflection symmetry and the center symmetry respectively except for the solid-phase of the nozzle flow. The solid particles collide with walls and with other particles at the center axis in an elastic collision fashion. The upstream boundary conditions for both cases are given by the characteristic curve method assuming that the flow is subsonic. The downstream boundary conditions are; the second order extraporation at the boundary is applied when the flow velocity is faster than the speed of sound at that point; the extraporating velocity is applied while the initial values of density and temperature are set at the outside boundary values when the flow velocity is between the speed of sound and zero; and the initial values of all variables are set when the flow velocity is zero or negative.

Results and Discussion

The numerical analysis of the particle laden two-phase nozzle and jet flow is performed to validate the present code. To do this, the experimental results (Ref. 12) are compared with the present numerical results. Especially the Lagrangian formulation of solid-phase flow gives an improved results in the solid particle profiles comparing with the results by the Eularian formulation.

Two-Phase Nozzle Flow

The cylindrically two-dimensional two-phase nozzle flow is simulated using the Flux Vector Splitting – Upwind scheme for the gas-phase and the Lagrangian formulation for the solid-phase. Although the particle collisions are not considered in the equations except for the center axis, the numerical results explain the experimental data of the two-phase nozzle flow.

Fig. 2 shows the case of the nozzle flow with the exit gaseous Mach number of 0.2 and with the solid particle diameter of $2\mu m$. In this case the flow does not choke at the nozzle throat; Fig. 2-(a) solid particle stream lines and (b) solid particle density profiles. The small particles follow the gas stream and do not collide with the nozzle wall.

Fig. 3 shows the case of the same nozzle flow with the exit Mach number of 0.2 and the solid particle diameter of $24\mu m$. In this case the solid particles collide with the nozzle wall and the particle does not follow the gas stream. However the gas stream lines in both cases do not get much effects from the solid particles.

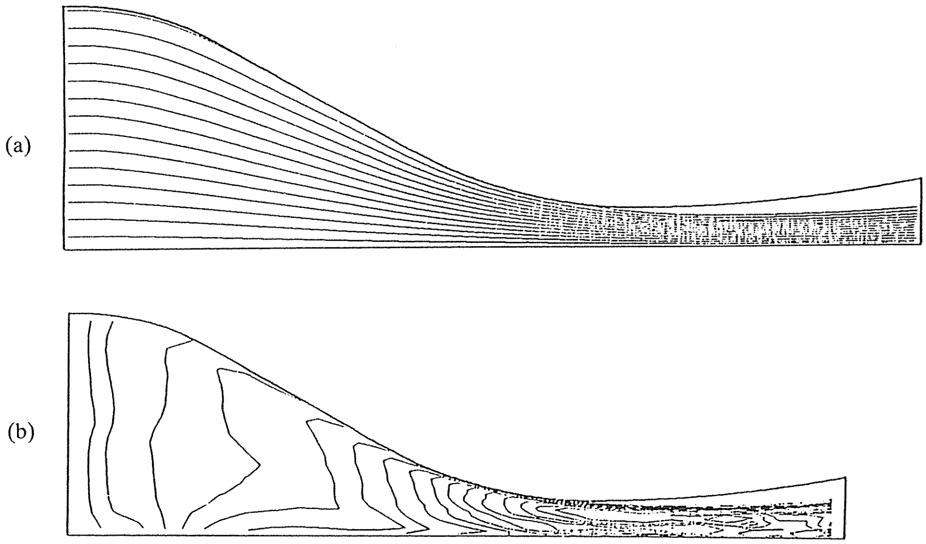

Fig. 2. The numerical results of the nozzle flow with the exit gaseous Mach number of 0.2 and with the solid particle diameter of 2μm ; (a) solid particle stream lines and (b) solid particle equi-density profiles.

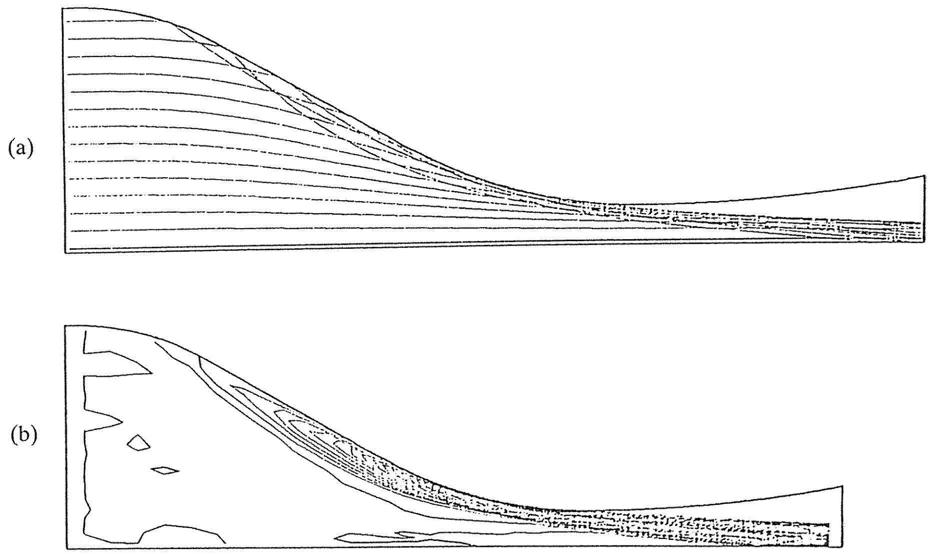

Fig. 3. The numerical results of the nozzle flow with the nozzle exit gaseous Mach number of 0.2 and with the solid particle diameter of 24μm ; (a) solid particle stream lines and (b) solid particle equi-density profiles.

Fig. 4 shows the solid particle concentration profiles at the exit of the nozzle in the two-phase nozzle flow with the particle diameter of 2μm (Fig. 4-(a)) and that of 24μm (Fig. 4-(b)). The solid line in the figure is the present numerical result and the broken line is the experimental result (Ref. 12) in both cases. It can be understood that the bottom of the particle profile contains smaller particles than large particles.

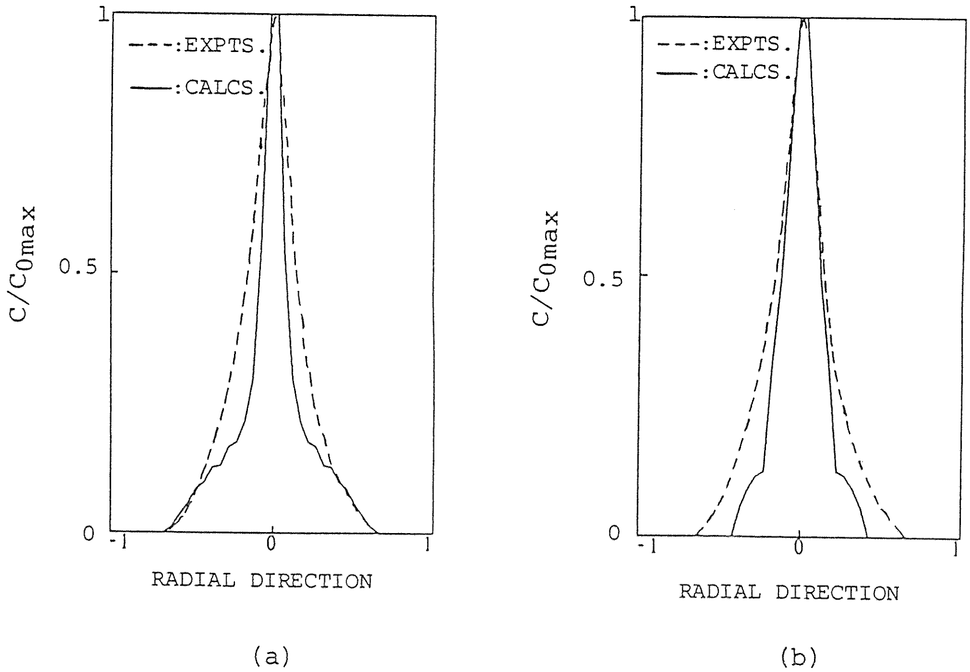

Fig. 4. The comparison between the numerical and experimental results of the solid particle radial concentration profiles at the nozzle exit in the two-phase nozzle flow with the particle diameter of (a) 2μm and (b) 24μm.

Two-Phase Jet Flow

The calculation of two-phase jet problems has been performed successfully elsewhere (Ref. 11). The previous study deals with the completely expanded flow. This means that the Eulerian formulation can simulate the cylindrical two-phase flow without any difficulty at the symmetric axis when the flow is expanding from the axis. The present calculation shows the flow is still slightly moving towards the axis, hence the Lagrangian type of calculation is used for the two-phase jet flow too.

Fig. 5 shows a comparison between the experimental and numerical results of particle concentration profiles in the two-phase jet flow. The particle size distribution is taken care of in the present numerical result to get a closer simulation of the experimental jet flow; seven parcent of 10μm, twenty six parcent of 18μm , thirty seven parcent of 24μm and thirty parcent of 36μm diameter particles (the average size of this distribution is about 24μm) are considered to simulate the problem. This computed results simulate the experimental results qualitatively and considerably quantitatively. In this case the particles

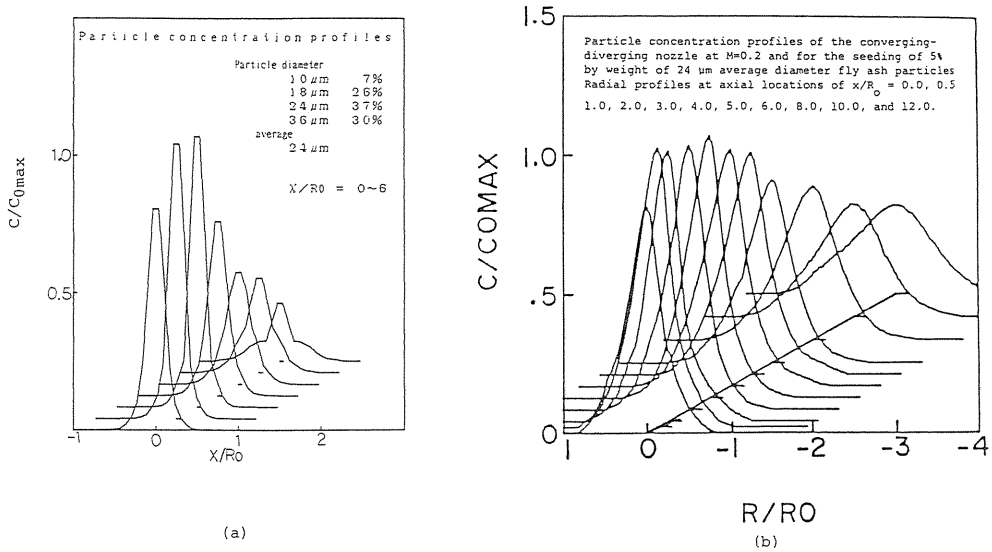

Fig. 5. The comparison between the numerical (a) and experimental (b) results of the solid particle radial concentration profiles of the two-phase jet flow at the locations of R_0, $2R_0$, $3R_0$, $4R_0$, $5R_0$, and $6R_0$ from the nozzle exit.

concentrate the most at the axis of the three radius distance further downstream.

Conclusions

The present numerical simulation of particle laden two-phase nozzle and jet flows can reach the following conclusions:

(1) The developed code is validated to simulate the gas-solid two-phase flow problems.
(2) The Eulerian formulation of a two-phase flow system provides the simpler structure and handles of equations well than does the Lagrangian formulation. However it depends on the boundary conditions such as that of the symmetric axis in the cylindrical case, where the Lagrangian method treats the problem better.
(3) The present simulation is the one that the solid particles are laden very lightly, so the gas-phase flow does not get much effect from the solid-phase whereas, in general, the gas-phase is strongly affected by the solid-phase flow.

References

1) Carrier, G.F., "Shock Waves in a Dusty Gas," J. of Fluid Mechanics, Vol. 4, March 1958, pp. 376–383.
2) Rudinger, G., "Some Effects of Finite Particle Volume on the Dynamics of Gas-Particle Mixtures," AIAA Journal, Vol. 3, No. 7, July 1985, pp. 1217–1222.

3) Marble, F.E., "Dynamics of Dusty Gases," Annual review of Fluid Mechanics, Vol. 2, Annual Reviews, Inc., 1970, pp. 397–446.
4) Marconi, F., Rudman, S., and Calia, V., "Numerical Study of One-Dimensional Unsteady Particle-Laden Flows with Shocks," AIAA Journal, Vol. 19, No. 10, Oct. 1981, pp. 1294–1301.
5) Chang, I.-S., "One- and Two-Phase Nozzle Flows," AIAA paper No. AIAA-80-0272, AIAA 18th Aero. Science Meeting, 1980, Pasadena CA.
6) Sommerfeld, M., "Numerical Simulation of Supersonic Two-Phase Gas-Particle Flows," Proc. of the 16th Int. Symp. on Shock Tubes and Waves, Aachen 1987, p. 235–241.
7) Carlson, D.J. and Hoglund, R.F., "Particle Drag and Heat Transfer in Rocket Nozzles," AIAA Journal, Vol. 2, No. 11, 1964, pp. 1980–1984.
8) Walsh, M.J., "Drag Coefficient Equations for Small Particles in High Speed Flows," AIAA Journal, Vol. 13, 1975, pp. 1526–1528.
9) Henderson, C.B., "Drag Coefficients of Sphere in Continuum and Rarefied Flows," AIAA Journal, Vol. 14, No. 6, 1976, pp. 707–708.
10) Steger, J.L. and Warming, R.F., "Flux Vector Splitting of the Inviscid Gasdynamic Equations with Application to Finite-Difference Methods," J. of Computational Physics, Vol. 40, 1981, pp. 263–293.
11) Hayashi, A.K., Matsuda, M., Fujiwara, T., and Arashi, K., "Numerical Simulation of Gas-Solid Two-Phase Nozzle and Jet Flows," AIAA Paper No. AIAA-88-2627, June 1988.
12) Hayashi, A.K., "Measurement and Calculation of Properties of Gas-Solid Two-Phase Jets," Ph.D. Thesis, University of Colorado, Dept. of Mechanical Engineering, 1980.